24th INTERNATIONAL CONGRESS ON SOUND AND VIBRATION
23–27 July 2017, London

SOUND ABSORBING PERFORMANCE OPTIMIZATION BASED ON CHARACTERISTIC IMPEDANCE

Zhehao Huang and Xiaolin Wang

Laboratory of Noise and Vibration Research, Institute of Acoustics, Chinese Academy of Sciences, Beijing 100190, China
email: wangxl@mail.ioa.ac.cn

A method is proposed for calculation and optimization of sound absorbing performance at low frequencies by choosing an optimal combination of multilayer porous materials, according to their characteristic impedance and propagation constant as two controlling material properties. First, a two-microphone two-load transfer function method according to ISO 10534-2 has been used to obtain the characteristic impedance and propagation constant, where geometrically asymmetrical or multilayer materials can be handled by an equivalent complex characteristic impedance. Second, this material characterization is verified by a direct measurement for various multilayer materials mounted with a hard termination. Last, optimization is performed to obtain the best possible low-frequency sound absorbing performance by comparing combinations of various lengths and characteristic impedances of multilayer materials with a given overall thickness. One advantage of using this method is when a best possible sound absorber needs to be constructed given a collection of realistic materials, with which a suitable theoretical model is yet to be associated, let alone their unknown parameters such as porosity, airflow resistivity and characteristic lengths. This method can be applied in designing preferable sound absorbers, and materials as well if further explored.
Keywords: porous materials, characteristic impedance, optimization

1. Introduction

Sound absorbing porous materials are widely applied in building, transportation, and other industries for noise reduction. However, we often encounter such difficulties in practice as what material to choose or what material model to apply. Apart from practical indices such as NRC (Noise Reduction Coefficient), it is quite often in literature that sound absorption coefficient is plotted against frequencies to demonstrate sound absorbing performance of a material. These data are usually obtained with test materials being of various thicknesses and mounting conditions. As absorption coefficient is affected by thickness and mounting conditions, it is hardly convenient to compare these materials. In addition to this, there are numerous models for various materials, either rigid, limpid, elastic or visco-elastic; or fibrous, granular, or foam materials. Some models depend only on a single parameter, while others depend on multiple parameters. For the latter, it is sometimes not easy to have all the needed material-model-dependent parameters. Assuming we have material samples with different thicknesses which cannot be altered, and there are materials in the literature where either absorption coefficient curves or NRCs are given but derived from various thicknesses or mounting conditions, what if we need compare and utilize these materials? Even if these materials are with the same thickness and mounting conditions, as well as airflow resistivities around the same order, would their sound absorption be similar, if not, then how?

For measuring sound absorption coefficient of a material, ISO 10534-2 standard of the two-microphone transfer-function method [1] has been widely applied. Based on this method, Utsuno *et*

al [2, 3] introduced a two-microphone two-cavity-load method (2M2L) for obtaining the complex characteristic impedance and propagation constant.

For calculating sound absorption coefficient, complex characteristic impedance and propagation constant, there are numerous models in the literature with one or more material parameters. The Delany-Bazley model [4] and the Allard-Champoux model [5] requires only one parameter, i.e. airflow resistivity. The Johnson-Allard model [6], the Biot-Allard model [6] and the Zwikker-Kosten model [7] have multiple parameters. Each of these models is generally valid for a specific range of materials: e.g. some for fibrous, some for rigid.

For sound absorption optimization, it is generally to calculate absorption based on material-model-dependent parameters, and to optimize these parameters for the desired absorption. Mechel *et al* [8] introduced two dimensionless parameters to combine the effects of frequency, airflow resistivity and sample thickness, then devised design charts for both monolayer and multilayer absorbers. For regularly arranged multilayer fibrous materials, Liu and Chen *et al* [9, 10] applied the Johnson-Champoux-Allard model for the computation of parameters and absorption optimization. Meng *et al* [11] studied gradient distributions of porosity and fibre diameters for optimization of multilayer absorbers. Zhang *et al* [12] applied a simulated annealing genetic arithmetic program for multilayer absorbers to find optimal combinations of seven material parameters.

Characteristic impedance and propagation constant are two primary material parameters which can substitute for all the material-model-dependent parameters. These two can be easily obtained with an impedance tube, then sound absorbing performance can be worked out no matter what thickness and mounting conditions or what a material model should be applied. This is especially helpful in comparing differences between materials and in optimizing a multilayer absorber. Here in this article, this impedance based method is applied so that we can optimize its performance even if an absorber is limited in a constricted space.

2. Impedance based method

2.1 Monolayer absorbers

Assuming that a plane wave propagates along $+x$ direction, a test material with thickness d is mounted on a hard termination in Fig. 1. The reference surface is set at the front of the test material. Microphones 1 and 2 are mounted at x_1 and x_2. Pressures p_1 and p_2 are the Fourier Transforms of time domain sound pressures at x_1 and x_2. Their transfer-function H_{12} is defined as

$$H_{12} \equiv \frac{p_2}{p_1}. \tag{1}$$

The complex reflection coefficient r and sound absorption coefficient α can be calculated

$$r = \frac{H_{12} - e^{-jk_0 s}}{e^{jk_0 s} - H_{12}} e^{2jk_0 x_1}, \quad \alpha = 1 - |r|^2 \tag{2}$$

where $j = \sqrt{-1}$ and $s = x_2 - x_1$.

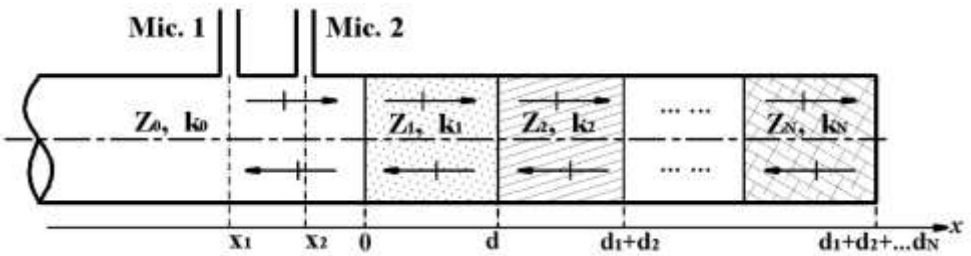

Figure 1: Sketch of a multilayer absorber in an impedance tube. Sound source is mounted on the left and absorber mounted on a hard termination on the right.

The 2M2L method is applied to calculate complex characteristic impedance Z and propagation constant k, while the two-cavities are substituted with one a hard termination and the other a cavity of depth L [13]. Impedance Z and propagation constant k can be obtained as follows:

$$Z = \sqrt{z_0' z_0 - z_0' z_1' + z_0 z_1'}, \quad k = \frac{1}{j2d} \ln\left(\frac{z_0 + Z}{z_0 - Z}\right) \tag{3}$$

where $z_0 = Z_0(1+r)/(1-r)$, $z_1' = -jZ_0 \cot(k_0 L)$ are the specific acoustic impedances at the sample front and back, respectively, Z_0 is the characteristic impedance of air, while variables with an apostrophe (') denoting ones with air cavity.

2.2 Multilayer absorbers

Assuming there are N layers of materials, by applying the continuity of pressure and particle velocity of sound at the interface between layers m and (m+1) $(\mathrm{m} = 1, 2, \ldots, \mathrm{N}-1)$, we obtain r_m from

$$\frac{1 + r_m e^{j2k_m \sum_{i=1}^{m} d_i}}{1 - r_m e^{j2k_m \sum_{i=1}^{m} d_i}} Z_m = \frac{1 + r_{m+1} e^{j2k_{m+1} \sum_{i=1}^{m} d_i}}{1 - r_{m+1} e^{j2k_{m+1} \sum_{i=1}^{m} d_i}} Z_{m+1}. \tag{4}$$

Substituting m from N-1 to 1, we can have r_1 by recursion, and the sound absorption coefficient

$$\alpha = 1 - \left|\frac{z_1 + Z_0}{z_1 - Z_0}\right|^2 \tag{5}$$

where $z_1 = Z_1(1+r_1)/(1-r_1)$ is the specific acoustic impedances at the front of first sample towards sound source and Z_1 is the complex characteristic impedance of first sample.

We can also assume an equivalent complex characteristic impedance and an equivalent propagation constant of a multilayer absorber the same as that of a monolayer absorber. This equivalence ensures that sound propagation properties outside the two absorbers are the same and their specific acoustic impedances at the front and back surfaces are also the same between the two absorbers.

2.3 Sound absorption optimization indices

Here the optimization is to search a maximum of an index, either noise reduction coefficient NRC, sound absorption average α_m, or optimal index Q [14], given a fixed overall thickness of a multilayer absorber mounted on a hard termination in an impedance tube. The noise reduction coefficient NRC is the average of the absorption coefficients in the 200 to 2500Hz 1/3 octave bands, as of standard ASTM C423-09a [15], measured in a reverberation room. Here we use a conversion relation [16] between what is measured in a reverberation room and what in an impedance tube to convert our measured absorption coefficients. The sound absorption average α_m is a rating for a geometric average of sound absorption coefficients over a frequency range $[f_{\min}, f_{\max}]$, 200-6400Hz here. The optimal index Q is defined as

$$Q \equiv \frac{1}{(1-\alpha_0)\Delta f} \int_{f_{\min}}^{f_{\max}} \alpha df - \alpha_0 \Delta f \tag{6}$$

where α_0 is an expected absorption coefficient in the frequency range $[f_{\min}, f_{\max}]$, $\Delta f = f_{\max} - f_{\min}$. The whole frequency range in this article is then divided into three parts with 1/3 octave bands: 200-708Hz, 708-2819Hz and 2819-6400Hz. Accordingly, their rating index Q are denoted as Q_L, Q_M and Q_H for low-, mid- and high-frequency indices, respectively.

2.4 Verification

To verify the characteristic impedance method for multilayer absorbers, we first measured characteristic impedance and propagation constant of each layered material, then derive their impedance

then sound absorption coefficients when they packed up as a multilayer absorber mounted on a hard termination. We then directly measured their sound absorption coefficients using the transfer function method. Fig. 2(a) shows calculated results agree well to directly measured ones.

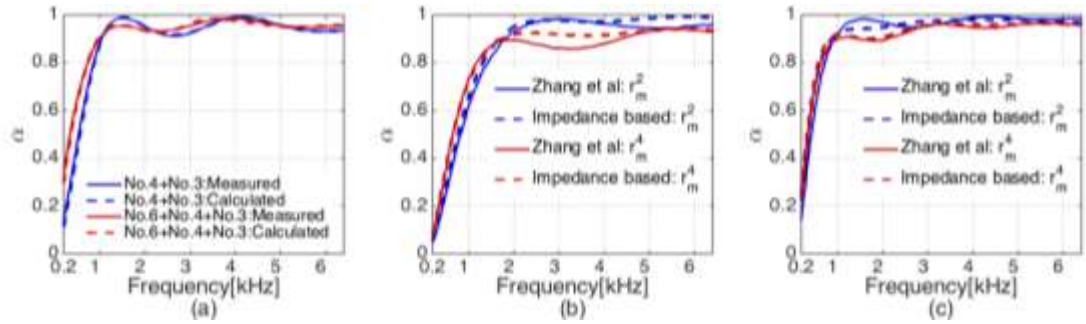

Figure 2: (a) Comparison between calculation and measurement, (b) (c) Comparison between optimization methods in this paper and in [12] using minimums of average r_m^2 and r_m^4, d = 25mm and d = 50mm.

To verify the impedance-based optimization method for multilayer absorbers, results are compared between one derived here based on characteristic impedance and another one [12] based on material-model-dependent parameters. Here we assume results derived in [12] use the same set of materials in [17], where we can derive needed characteristic impedance and propagation constant. Figure 2(b) and (c) shows comparisons by the same rating indices used in [12]. Parameter r_m represents the mean complex reflection coefficient in the frequency range 200-6400Hz. Optimization based on a minimum of average r_m^2 is basically equivalent to a maximum of sound absorption average α_m. This figure shows that the impedance-based method can achieve the same level of optimization as the material-model-dependent method.

3. Results and discussions

Six samples of various materials were used for comparison and optimization. Their measured properties are listed in Table 1. The airflow resistivity σ was measured by an in-house apparatus, porosity Ω, pore-size average S_p, pore-size distribution, and surface to volume ratio BS/BV were measured by a SCANCO micro-CT scanner, while impedance, propagation constant and sound absorption were measured by a B&K Type 4206 impedance tube with a valid frequency range 200-6400Hz. In the impedance measurement, cavity depth L was set to 20mm to avoid resonance.

3.1 Comparison between materials

In order to observe effects caused by material itself rather than boundary conditions and absorber structure, materials need to have the same thickness and mounting condition. By directly measuring the characteristic impedance and propagation constant of materials in Table 1, Fig. 3 shows calculated sound absorption coefficients of the materials with the same thickness d = 20mm mounted on a hard termination.

Between materials in Fig. 3 we can see that sample No. 2 melamine shows a better sound absorbing performance at high frequencies, No. 6 steel fibres shows a better performance at low frequencies, while other materials show different absorption peaks in the mid-frequency range. Table 1 has also listed the sound absorption average α_m of these materials. It is shown that the absorption coefficient average of most materials are around 0.7, but their absorption coefficient curves differ widely, e.g. No. 2 melamine and No. 3 polyurethane, even if their resistivities are around the same order. This shows resistivity alone may not be able to characterize their sound absorbing performance for certain materials. Although samples No. 1 rubber crumbs and No. 4 steel fibres have similar surface to volume ratios, the former has a much narrower absorption frequency range than the latter. A further observation reveals that the pore-size distribution of the former is much narrower than the latter as well. This indicates that, for sound absorption, pore-size distribution is likely to

contribute significantly to the frequency range which a material can effectively absorb. A more detailed analysis of comparison between granular, foam and fibrous materials is to be presented in a separate paper.

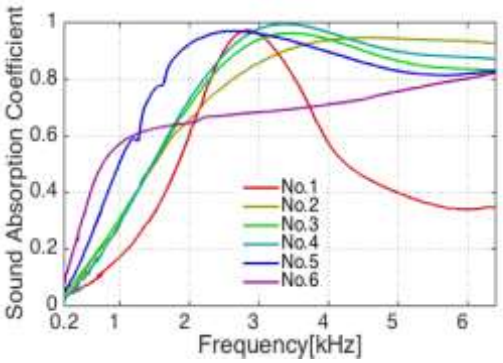

Figure 3: Calculated absorption coefficients of materials with thickness d = 20mm on a hard termination.

Table 1: Measured properties of materials

Sample No.	1	2	3	4	5	6
Material	Rubber crumbs	Melamine foam	Polyurethane foam	Steel fibres	Wood fibres	Steel fibres
σ [$\times 10^4$ Pa·s/m^2]	0.822	1.59	1.79	2.75	4.69	13.6
Ω [%]	64.75	98.55	94.29	84.63	92.41	91.95
BS/BV[1/mm]	30.40	329.3	131.6	50.96	158.6	176.7
S_p [mm]	0.4284	0.1886	0.2534	0.2394	0.1418	0.0845
α_m (d = 20mm)	0.48	0.69	0.71	0.70	0.75	0.66

Table 2: Optimization values of various rating indices

Overall thickness[mm]	Q_L	Q_M	Q_H	NRC	α_m
20	-0.97	0.51	0.98	0.50	0.81
40	-0.21	0.88	0.99	0.80	0.89
60	0.22	0.95	0.99	0.85	0.92

3.2 Optimization

3.2.1 Sound absorption coefficient

Sound absorption coefficient curves based on various rating indices and overall thicknesses for three-layer absorbers made of materials in Table 1 are given in Fig. 4(a). Optimal values of performance indices Q, NRC and α_m for each overall thickness are listed in Table 2. For Q ratings, the expected sound absorption coefficient α_0 is set to 0.65.

It is shown in Fig. 4(a) that for Q_L, Q_M and NRC based optimization, sound absorbing performance is enhanced at mid and low frequencies, but reduced at high frequencies. This high-frequency range can be called a 'compromised' range. For Q_H and α_m based optimization, sound absorbing performance is relatively enhanced in the whole frequency range, especially at high frequencies. As the overall thickness increasing, all the indices increase except Q_H almost remains constant. Meanwhile, increments of Q_L, Q_M decrease. This means that the absorber then behaves like being infinitely thick. After a certain thickness has been reached, it is much harder to enhance the sound absorbing performance by simply increasing the overall thickness at high frequencies. Values $Q_L < 0$ in Table 2 means the performance at low frequencies cannot reach the expectation. This shows how difficult it is to enhance performances of thin absorbers at low frequencies due to the 1/4 wavelength rule. This also shows the NRC based optimization is more likely to enhance sound absorption at mid- to low- rather than high-frequencies, as suggested by the chosen centre frequencies of the listed materials in Table 1 with 20mm thickness, the absorption coefficient average of an optimized multilayer absorber can be improved from 0.75 of their best monolayer absorber to 0.81.

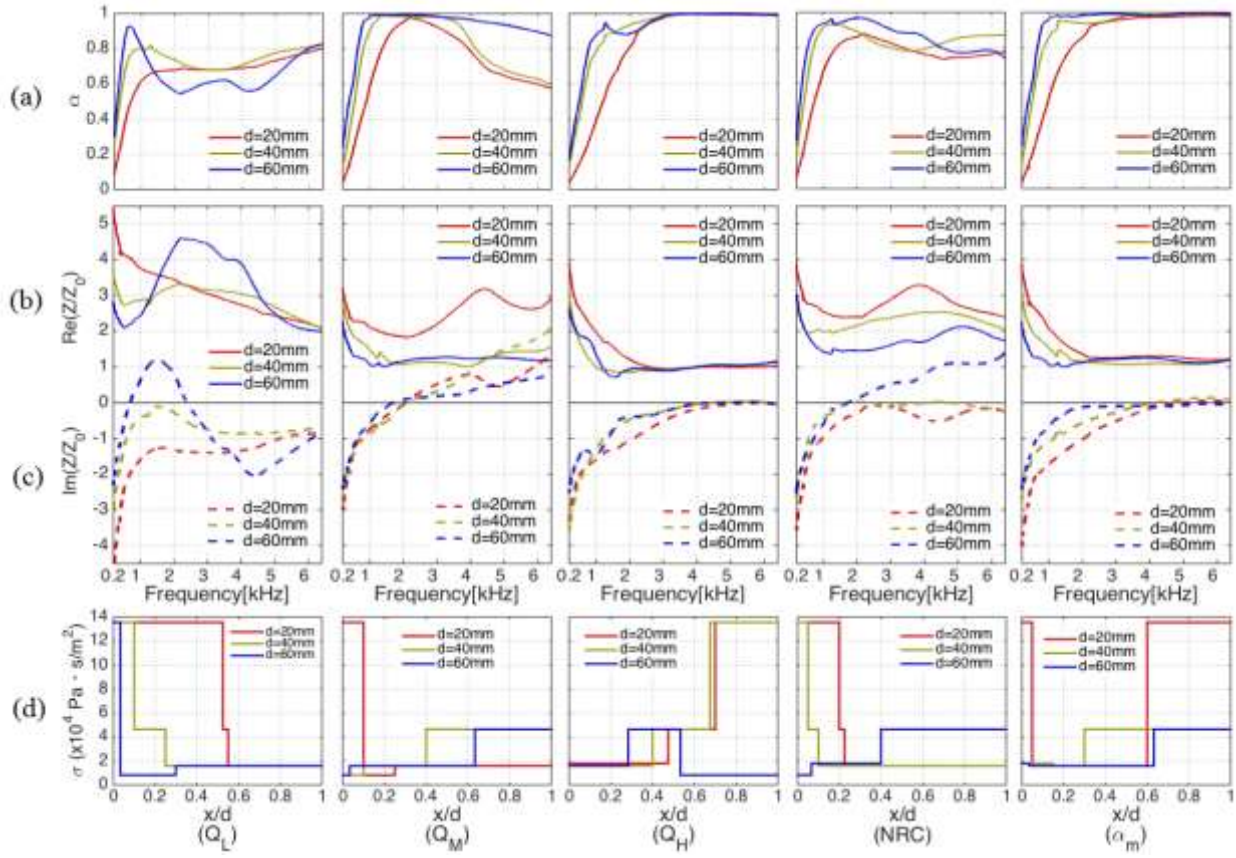

Figure 4: Optimization results for indices Q_L, Q_M, Q_H, NRC and α_m, (a) Sound absorption coefficient, (b) $\mathrm{Re}\left(Z/Z_0\right)$, (c) $\mathrm{Im}\left(Z/Z_0\right)$, (d) Airflow resistivity distribution.

3.2.2 Effects of equivalent characteristic impedance

For multilayer absorbers, the equivalent characteristic impedance provides a way to look into the overall acoustic property of the absorber as a whole in the frequency domain, shown in Fig. 4(b) and (c).

For an ideally high sound absorption coefficient, the real part of characteristic impedance needs to be close to 1 while the imaginary part to 0. Although characteristic impedances vary according to different optimization indices, they show similar tendencies for the same index. Their real parts in the concerned frequency range are relatively lower and smoother than in the other frequency ranges. In the 'compromised' ranges, their real parts tend to deviate significantly from the ideal value. For the NRC based optimization, thinner absorbers such as *d* = 20mm and 40mm show a similar 'compromised' range as of the Q_L based optimization, while thicker absorbers such as *d* = 60mm shows a similar 'compromised' range as of the Q_M based optimization. Degrees of deviation from ideal characteristic impedance indicate how hard to be able to achieve the intended optimization. Comparing with all the rating indices here, although the Q_L based optimization can most effectively raise sound absorption at low end frequencies, the α_m based optimization is the most efficient one to raise overall absorption covering the whole range of frequencies. The degree of 'deviation' shows for an absorber how weak a frequency range is. This would help for further tuning in optimization.

3.2.3 Effects of airflow resistivity distribution

While the equivalent characteristic impedance representing an overall quality of a multilayer absorber, airflow resistivity distribution would show in more detail what characteristics lay inside each layer. The airflow resistivity σ is a material parameter independent of both sample thickness and surface area normal to the incident sound, but significantly affecting sound absorbing performance. The distribution of the resistivity along the thickness is shown in Fig. 4(d).

For the Q_L based optimization, contradictory to the usual assumption that the airflow resistivity starts with a small value on the front side and increases towards the backing wall [8], our result shows an airflow resistivity on the front with a relatively higher value than the following layer, then the value decrease towards the backing. The structure of a front layer with a relatively high airflow resistivity can be regarded as a micro-perforated screen, together with the lower resistivity layers as a Helmholtz resonator. For Q_H and α_m based optimization, the airflow resistivity shows generally an ascending order, increasing from the front layer towards the back, in accord with results in [8]. Distributions for the Q_M based optimization are generally between Q_L and Q_H, sometimes with a high resistivity layer shifting towards the middle or back. For the NRC based optimization, thinner absorbers have similar distributions as Q_L based optimization while thicker absorbers have similar distributions as the Q_M based optimization, a trend in accord with that of the equivalent characteristic impedance. It shows that a third layer at the back with an increased resistivity may also enhance sound absorption.

4. Conclusion

In this paper, sound absorption of multilayer absorbers is optimized based on the characteristic impedance and propagation constant instead of material-model-dependent parameters. In comparison with fibrous and foam materials, granular porous materials tend to have a narrower band and lower sound absorption performance. Results indicate that, for sound absorption, the surface to volume ratio may contribute to a certain extent to resistivity. It seems that pore-size distribution will significantly affect the width of frequency range where sound is effectively absorbed. Employing performance rating indices *Q*, NRC and α_m, our optimization shows that individual rating index is tailored by a preferred frequency range. Although low frequency absorption can be raised by Q_L, it is nevertheless achieved by the sacrifice of absorption at mid to high frequencies. The NRC based optimization is more likely to raise sound absorption at mid- to low- rather than high-frequencies. An index like NRC but covering a wider range of 1/3 octave bands like α_m would enable a better sound absorption capability. By examining the airflow resistivity distribution, a multilayer absorber having a front layer with a relatively high airflow resistivity can behave like a micro-perforated screen, together with a lower resistivity layer behind as a nonlocal Helmholtz resonator. A further third layer with a slightly increased resistivity can be placed at the back to increase sound absorption. An absorber constructed this way is likely to lead to a good absorption performance at low frequencies.

ACKNOWLEDGEMENTS

The authors gratefully acknowledge the support from the National Natural Science Foundation of China (No. 11574344) and the National Basic Research Program of China (No. 2011CB610302, No. 2012CB720203). We would like to thank Qingbo Ao of the Northwest Institute for Nonferrous Metal Research for providing steel fibres.

REFERENCES

1 *Acoustics - Determination of sound absorption coefficient and impedance in impedance tubes - Part 2: Transfer-function method*, ISO standard 10534-2:2001, (2001).

2 Utsuno, H., Tanaka, T. and Fujikawa, T. Transfer function method for measuring characteristic impedance and propagation constant of porous materials, *Journal of Acoustical Society of America*, **86** (2), 637-643, (1989).

3 Utsuno, H., Wu, T. W., Seybert, A. F. and Tanaka, T. Prediction of sound fields in cavities with sound absorbing materials, *AIAA Journal*, **28** (11), 1870-1876, (1990).

4 Delany, M. E. and Bazley, E. N. Acoustical properties of fibrous absorbent materials, *Applied Acoustics*, **3** (2), 105-116, (1970).

5 Allard, J. F. and Champoux, Y. New empirical equations for sound propagation in rigid frame fibrous materials, *Journal of the Acoustical Society of America*, **91** (6), 3346-3353, (1992).
6 Allard, J. F. and Atalla, N. *Propagation of Sound in Porous Media: Modelling Sound Absorbing Materials*, 2nd ed., John Wiley & Sons, Chichester, West Sussex, (2009).
7 Zwikker, C. and Kosten, C. W. *Sound Absorbing Materials*, Elsevier, New York, (1949).
8 Mechel, F. P. Design charts sound absorber layers, *Journal of Acoustical Society of America*, **83** (3), 1002-1013, (1988).
9 Liu, S., Chen, W. and Zhang, Y. Design optimization of porous fibrous material for maximizing absorption of sounds under set frequency bands, *Applied Acoustics*, **76**, 319-328, (2014).
10 Chen, W., Liu, S., Tong, L. and Li, S. Design of multi-layered porous fibrous metals for optimal sound absorption in the low frequency range, *Theoretical and Applied Mechanics Letters*, **6** (1), 42-48, (2016).
11 Meng, H., Ao, Q., Tang, H., Xin, F. and Lu, T. Dynamic flow resistivity based model for sound absorption of multi-layer sintered fibrous metals, *Science China Technological Sciences*, **57** (11), 2096-2105, (2014).
12 Zhang, B., Zhang, W. and Zhu, J. Optimization of sound absorbing performance for gradient multi-layer-assembled sintered fibrous absorbers, *Proceedings of SPIE* 8409, Third International Conference on Smart Materials and Nanotechnology in Engineering, 84090C, (2012).
13 Larner, D. J. and Davy, J. L. Prediction complex chracteristic acoustic impedance, *Proceedings of the 43rd International Congress on Noise Control Engineering*, Melbourne, Australia, 16-19 November, (2014).
14 Wang, X. and Lu, T. Optimized acoustic properties of cellular solids, *Journal of Acousicalt Society of America*, **106** (2), 756-765, (1999).
15 *Standard Test Method for Sound Absorption and Sound Absorption Coefficients by the Reverberation Room Method*, ASTM C423-09a, (2009).
16 Ma, D.Y. and Shen, H. *Handbook of Acoustics* (in Chinese), Science Press, Beijing, (2004).
17 Zhang, B. and Chen, T.N. Calculation of sound absorption characteristics of porous sintered fiber metal, *Applied Acoustics*, **70** (2), 337-346, (2009).